Series DC Arc Fault Detection Method for PV Systems Employing Differential Power Processing Structure

Hwa-Pyeong Park, *Member, IEEE*, Mina Kim, *Student Member, IEEE*, Jee-Hoon Jung, *Senior Member, IEEE*, and Suyong Chae, *Member, IEEE*

***Abstract*—Arc fault detection is an important process for ensuring the safety of PV and grid-connected inverters and is essential for producing PV systems in real applications. However, it is difficult to detect series dc arc faults using conventional fuses because these faults produce only small current variations. In addition, the arc fault detection devices have limited performance, because they focused on arc fault detection between PV arrays and inverter. Moreover, they require the additional current and voltage sensors to implement the arc fault detection algorithm. This article proposes an arc fault detection algorithm employing differential power processing (DPP) structure. The proposed algorithm only uses intrinsic voltage sensors of DPP and inverter, which can improve the cost-effectiveness of PV systems. In addition, the proposed algorithm can integrate the functionality of maximum power processing for each PV panel and arc fault detection. The voltage relationship between DPP and inverter is analyzed to detect the arc fault condition according to the DPP voltage sensing type. The performance of DPP units and its voltage relationship are verified with the control hardware-in-the-loop system. The arc fault detection performance is verified with the prototype PV system.**

***Index Terms*—Arc fault, dc–dc converter, photovoltaic.**

I. Introduction

THE renewable energy sources, such as photovoltaic (PV) and wind power, are continuously increasing to reduce the threat posed by environmental pollution [1]. Grid-connected renewable energy systems are widely used in decentralized power system and household, and hence, the interest in the safety of renewable power system and inverter is increasing [2]–[4]. PV systems are inherently dc sources, and dc arc faults are induced between PV panels and between a PV array and an inverter. The loose connector, damaged, and pitched power cable by aging, and cracked and corroded solder joint cause the series dc arc fault in PV systems. The arc fault circuit interrupter (AFCI) is necessary for ensuring the safety of inverters and PV systems. The Underwriters Laboratories (UL) develops UL 1699B standards to detect the arc fault condition [5]. In addition, the National Electrical Code (NEC) requires AFCI for all PV systems over 80 V [6].

The arc faults consist of series and parallel arc fault. In addition, the arc fault can be modeled as combination of R-L [7], [8]. The parallel arc fault can be easily detected because they cause a large current change [9], [10]. However, the series arc fault is different because it causes only a small current change, which is not sufficient to melt fuses. AFCI are effective in detection arc fault using several arc fault sensing methods. However, the arc fault can occur in various locations on the PV system. Fig. 1 shows the PV system structure and location where arc fault can occur [5]. Many AFCI are required to obtain the safety of PV systems, which can increase the cost of PV systems.

In previous studies, several algorithms have been developed for series dc arc fault detection. In [11]–[14], time domain analysis using current and voltage information was applied to detect the arc fault condition. Those methods use only a single

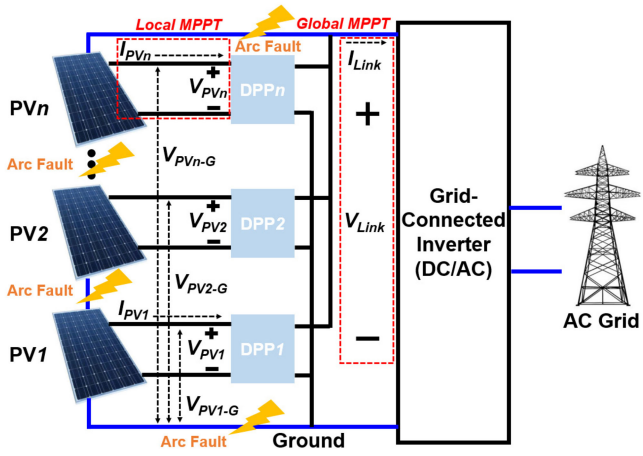

Fig. 1. PV system structure and various locations of the dc series arc fault.

Manuscript received September 3, 2020; revised January 20, 2021; accepted February 21, 2021. Date of publication February 25, 2021; date of current version June 1, 2021. This work was supported by the Framework of the Research and Development Program of the Korea Institute of Energy Research (C1-2420). Recommended for publication by Associate Editor J. Stauth. *(Corresponding author: Suyong Chae.)*

Hwa-Pyeong Park and Suyong Chae are with the Energy Efficiency Division, Korea Institute of Energy Research, Seoul 34129, South Korea (e-mail: hppark@kier.re.kr; sychae@kier.re.kr).

Mina Kim is with the Electrical Engineering, Ulsan National Institute of Science and Technology, Ulsan 44919, South Korea (e-mail: kmaop44@unist.ac.kr).

Jee-Hoon Jung is with the Electrical and Computer Engineering, Ulsan National Institute of Science and Technology, Ulsan 44919, South Korea (e-mail: jhjung@unist.ac.kr).

Color versions of one or more figures in this article are available at https://doi.org/10.1109/TPEL.2021.3061968.

Digital Object Identifier 10.1109/TPEL.2021.3061968

voltage or current sensor to detect the arc faults. Their simple detection circuit and algorithm provide fast fault detection but have poor noise immunity. The arc fault condition induces noise in range of several tens of kilohertz in the frequency domain. In [15]–[19], the fast Fourier transform (FFT) and short time Fourier transform are used to detect the arc fault condition. In [20]–[24], the discrete wavelet transform, and wavelet packet transform were introduced to detect the arc fault using a predefined threshold. Notably, these can obtain both time and frequency information and can implement multiresolution analysis through their window functions. In [25], a statistical method was introduced to detect arc fault condition, which uses statistics-based thresholds. The previous methods focus on the series dc arc fault detection between PV arrays and inverter. In [26]–[28], the machine learning was used to detect the arc fault condition. These methods can detect the arc fault condition with the consideration of several arc fault characteristics. However, the machine learning based algorithm has limited detection accuracy, which cannot ensure the safety of PV systems. In addition, this method requires much information using several sensing devices.

The conventional arc fault detection algorithm requires additional current and voltage sensors, which can degrade the cost-effectiveness of PV systems. In addition, the series dc arc fault between PV panels was not focused before compared to the arc fault between PV arrays and inverter. However, the arc fault detection between PV panels is necessary, because the series connected PV panels have same current rating with inverter. In the practical manner, therefore, many voltage and current sensors are required to detect all the arc faults of PV systems, which drastically reduce the cost-effectiveness.

Differential power processing (DPP) structure have been developed to obtain the maximum power point tracking (MPPT) for each PV unit [29]–[33]. Therefore, the main inverter and DPP operate at the global and local MPPT, respectively. Fig. 1 shows the PV systems employing the DPP structure. The DPP intrinsically measure each PV panel's voltage. This article proposes the functional integration of DPP structure with the MPPT operation and arc fault detection algorithm, which can improve the power generation efficiency and system safety. This method can detect the arc fault condition between PV panels and between PV array and inverter without the additional sensors. In addition, it proposes the arc fault detection method according to the voltage sensing method of DPP units, which can extend the functional usage. The detection algorithm uses the time and frequency domain analysis according to the arc fault condition. The performance of DPP unit and its voltage relationship are verified with control hardware-in-the-loop (Control-HIL) system. The arc fault detection performance is verified with the prototype PV system using the PV simulator, arc fault generator, arc fault detector, and grid-connected inverter.

II. Arc Fault Detection for DPP Structure

DPP units intrinsically measure the voltage of each PV panel, which can use two types of sensing methods: a differential type and a common ground type. Fig. 2(a) shows the differential type sensing method. The DPP units can directly measure each PV voltage, which can be described as follows:

$$V_{DPP1} = V_{PV1}, \ldots, V_{DPPn} = V_{PVn}. \tag{1}$$

The isolated differential voltage sensors are used to directly measure each PV voltage, which is a commonly used method for DPP units. This method can measure only PV voltages without other voltage drops. However, it is an expensive method as it uses isolated sensors. Fig. 2(b) shows the common ground type sensing method. The DPP units indirectly measure each PV voltage, which can be expressed as follows:

$$V_{DPP1} = V_{PV1-G}, \ldots, V_{DPPn} = V_{PVn-G} - V_{PV(n-1)-G}. \tag{2}$$

This method requires postprocessing to calculate each PV panel voltage. For example, the nth PV voltage can be measured with the ground to the nth PV voltage (V_{PVn-G}) and ground to the $n-1$th PV voltage ($V_{PV(n-1)-G}$). The nonisolated type sensors have high cost-effectiveness. However, in this method, the voltage drop caused by arc fault conditions on the measured

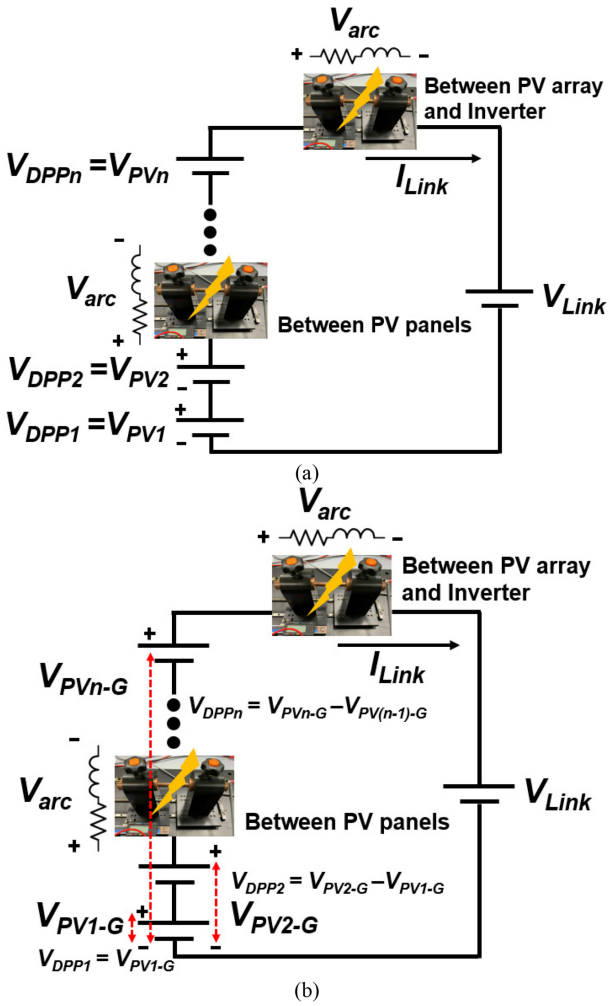

Fig. 2. Voltage measurement methods. (a) Differential type sensing. (b) Common ground type sensing.

PV voltage are also contained, which cannot be used to obtain the precise PV voltage. In this article, the dc-link voltage of inverter and each PV voltage measured by DPP units are used to detect the arc fault conditions.

A. Arc Fault Detection Using Differential Type PV Voltage Sensing Method

An arc fault can occur between PV panels or between PV arrays and an inverter. Fig. 2(a) shows the differential type sensing method with the equivalent circuit of PV systems including the arc fault condition. The sum of all series connected PV panel voltages is the PV array voltage, which can be calculated as follows:

$$V_{PV,tot} = V_{DPP1} + V_{DPP2} \cdots + V_{DPPn}. \tag{3}$$

In addition, the dc-link voltage of inverter can be derived while considering the (3) and arc fault condition as follows:

$$V_{Link} = V_{PV,tot} - V_{arc} \tag{4}$$

where V_{arc} is the voltage drop caused by the arc fault condition, which is determined with the arc fault impedance and current.

The arc fault impedance was modeled as R-L combination [7], [8]. Under no arc fault condition, (3) and (4) are ideally the same magnitude with zero V_{arc} value, which can be expressed as follows:

$$V_{PV,tot} = V_{Link}. \tag{5}$$

Under the arc fault condition, the total PV voltage is higher than the dc-link voltage of inverter according to (3) and (4); this relationship can be described as follows:

$$V_{PV,tot} > V_{Link}. \tag{6}$$

In the differential type sensing, the voltage of $V_{PV,tot}$, V_{arc}, and V_{Link} have to meet the Kirchhoff's voltage law. The voltage relationship of (5) and (6) can be satisfied under the arc fault conditions between PV panels or between PV arrays and an inverter. Fig. 3 shows simulation results of $V_{PV,tot}$ and V_{Link} values according to the arc fault and no arc fault conditions. The MPPT induces the PV voltage variation. The voltage relationship of (5) and (6) is verified according to the arc fault condition.

The detection precision can be improved with the consideration of the voltage drop in the line resistance, which can be described as follows:

$$V_{drop} = I_{Link} R_{line}. \tag{7}$$

This voltage drop according to the line resistance has variation according to the link current. The irradiation of PV, partial shading, and control algorithm of inverter induces the voltage drop variation of (7). Therefore, the consideration of line resistance can improve the arc fault detection precision between the arc fault condition and dc-link current variation. From (3), (4), and (7), the voltage relationship for the arc fault detection can be described as follows:

$$V_{PV,ave} - V_{drop} > V_{Link} \tag{8}$$

where $V_{PV,ave}$ is the moving average value of $V_{PV,tot}$. In the no arc fault condition, the voltage relationship can be described

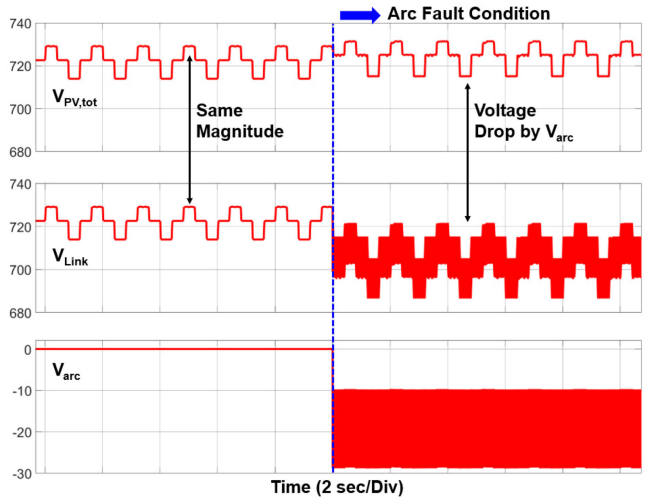

Fig. 3. Voltage comparison of $V_{PV,tot}$ and V_{Link}.

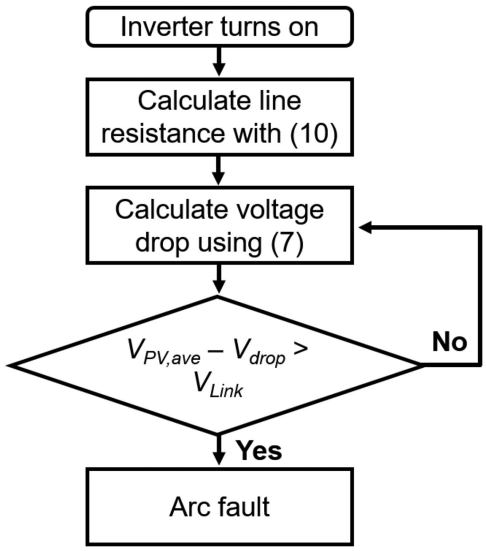

Fig. 4. Arc fault detection algorithm for differential type voltage sensing.

with (5) and (7) as follows:

$$V_{PV,ave} - V_{drop} = V_{Link}. \tag{9}$$

Fig. 4 shows the proposed arc fault detection algorithm for the differential type PV voltage sensing method. When the inverter is turned ON, the controller has a default line resistance value. The controller updates the line resistance by calculating (10) using the values of $V_{PV,tot}$, V_{Link}, and I_{Link} as follows:

$$R_{Line} = \left(V_{PV,tot} - V_{Link}\right) / I_{Link}. \tag{10}$$

Next, the voltage drops of (7) can be calculated using (10) and the dc-link current. The arc fault condition can be detected with the time domain relationship given in (8).

B. Arc Fault Detection Using Common Ground Type PV Voltage Sensing Method

Based on (2), the common ground type sensing method can be used to measure the voltage of each PV panel. In the case of an arc fault condition between PV arrays and an inverter, the total PV voltages can be the same as (3), because the voltage drop of an arc fault condition occurs between the total PV voltage and the dc-link voltage. Therefore, the arc fault condition between PV arrays and an inverter can be detected using the same relationship as the one between (8) and (9), which uses the same arc detection algorithm presented in Fig. 4.

In the case of an arc fault between PV panels, the calculated DPP voltages contain the voltage drop by the arc fault. The proposed algorithm in Fig. 4 cannot detect the arc fault condition, because $V_{PV,tot}$ and V_{Link} are the same at the arc fault condition. In this case, the total voltage of the PV panels can be described by considering the arc fault as follows:

$$V_{PV,tot} = V_{DPP1} + V_{DPP2} \cdots + V_{DPPn} - V_{arc}. \tag{11}$$

When the arc fault condition occurs between the *n*th PV panel and *n−1*th PV panel, the *n*th DPP voltage can be expressed as follows:

$$V_{DPPn} = V_{PVn-G} - V_{arc} - V_{PV(n-1)-G}. \tag{12}$$

Therefore, an additional arc fault detection algorithm is necessary for the arc fault condition between PV panels.

Based on (11) and (12), the measured DPP voltage contains the voltage drop caused by the arc fault condition, which has noise in the range of several tens of kilohertz [15]–[19]. The FFT analysis can be used to detect the arc fault condition by utilizing a fast computation speed to calculate the digital Fourier transform (DFT). The DFT of each DPP voltage can be derived as follows:

$$V_{DPP}[k] = \frac{1}{N}\left|\sum_{k=0}^{N-1} v_{DPP}[n]\, e^{-j2\pi kn/N}\right| \tag{13}$$

where $V_{DPP}[k]$ is the DPP voltage according to the frequency analysis, *k* is the frequency bin, and *n* is the number of sampling point, which can range from *0* to *N*. The frequency resolution is determined using the sampling frequency ($f_{sampling}$) and *N* and can be expressed as $f_{sampling}/N$. The number of complex DFT frequency components is defined as *N*/2.

In this experiment, the sampling frequency is 200 kHz and *N* is 1024. The designed FFT has 512 frequency bins with a 195 Hz frequency resolution. Since the range of the designed frequency analysis is from 10 to 70 kHz, the corresponding 52th–359th frequency bins are analyzed for arc fault detection. The controller calculates the FFT results of each PV panel using (13), which can be described according to the order of PV panels as $V_{DPP}[k, u]$, where *u* is the order of the PV panels. Fig. 5 shows the experimental FFT comparison between arc fault and no arc fault conditions for the designed frequency range. The relative comparison of FFT magnitude between PV panels can detect the arc fault condition, which is derived as follows:

$$V_{dif}[k,u] = V_{DPP}[k,u] - V_{DPP}[k,u-1] \tag{14}$$

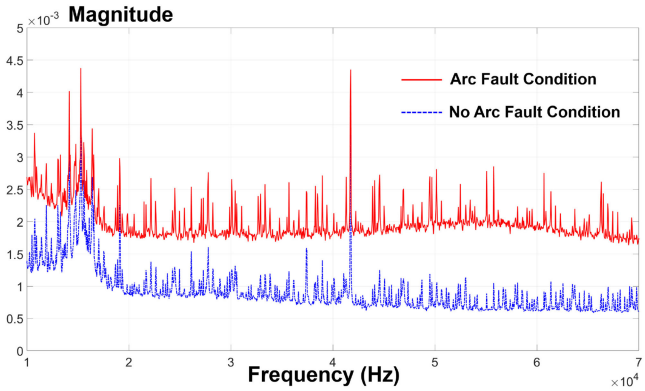

Fig. 5. FFT magnitude comparison according to the arc fault and no arc fault conditions.

$$V_{comp}[k,u] = \begin{cases} 1, & \text{if } V_{dif}[k,u] > 0 \\ 0, & \text{if } V_{dif}[k,u] <= 0 \end{cases} \tag{15}$$

where V_{dif} is the relative magnitude difference according to the PV panels and V_{comp} is the magnitude comparison of V_{dif}. The sum of V_{comp} according to the desired frequency range can be described as follows:

$$V_{c,t}[u] = \sum_{k=k_1}^{k_2} V_{comp}[k,u] \tag{16}$$

where k_1 and k_2 are the minimum and maximum frequency bins, respectively. The threshold value for $V_{c,t}$ to detect the arc fault condition can be defined as follows:

$$V_{th,freq} = \alpha_{th,freq}(k_2 - k_1),\ 0 < \alpha_{th,freq} < 1 \tag{17}$$

where $\alpha_{th,freq}$ is the adjustable threshold factor in (17). When $V_{c,t}$ is higher than the threshold value ($V_{th,freq}$), the arc fault can be detected using the frequency analysis.

The arc fault between PV panels induces the drastic voltage drop, which can be detected with the time domain analysis for implementing the frequency analysis. It can mitigate the computation burden of digital signal processor (DSP). The moving average of PV voltages and its standard deviation can be described as follows:

$$v_{aver,DPP}[u] = \frac{1}{U}\sum_{a=0}^{U-1} v_{DPP}[a,u] \tag{18}$$

$$v_{st,DPP}[u] = \sqrt{\frac{1}{U}\sum\nolimits_{a=0}^{U-1}\left(v_{DPP}[a,u] - v_{aver,DPP}[u]\right)^2} \tag{19}$$

where *a* is the number of moving average. Fig. 6 shows the standard deviation of each PV voltage based on the experimental results. The drastic voltage variation is detected using the time domain threshold ($V_{th,tim}$), which can be defined as follows:

$$v_{th,tim}[n] = v_{aver,st,DPP}[n] + \alpha_{th,tim} v_{st,DPP}[n] \tag{20}$$

where $v_{aver,st,DPP}$ is the moving average of standard deviation, $\alpha_{th,tim}$ is the adjustable threshold factor in (18), which can be designed in a statistical manner, for example, using three-sigma

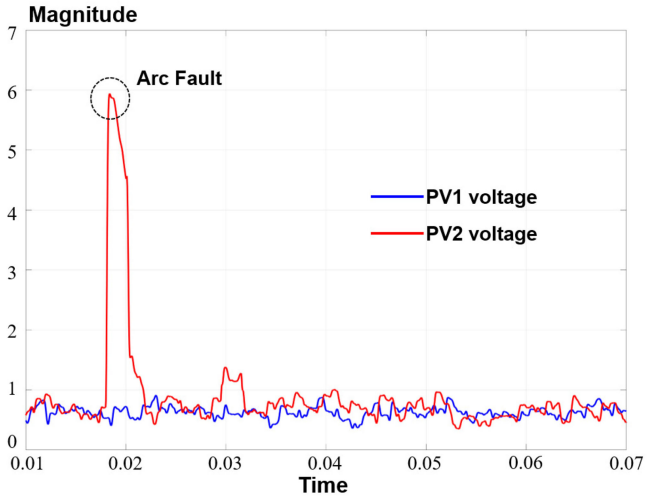

Fig. 6. Standard deviation of PV panel's voltage.

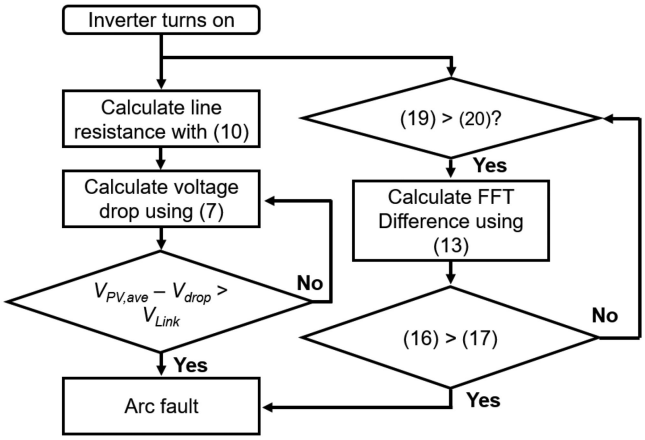

Fig. 7. Arc fault detection algorithm for common ground type voltage sensing.

rules. When the standard deviation is over the threshold value of time domain, the DSP calculates the FFT magnitude for comparison between PV panels. Notably, the PV voltage can be drastically changed by the partial shading or drastic irradiance variation. Therefore, the arc fault cannot be detected with only the time domain analysis. However, it can be useful factor to detect the arc fault condition for alleviating the computation burden of DSP. Fig. 7 shows the arc fault detection algorithm for the common ground type voltage sensing method. In the case of arc fault between PV arrays and inverter, the arc fault detection algorithm is same as the differential type sensing method. In the case of arc fault between PV panels, the time domain analysis detects the drastic voltage variation. After this detection, the relative comparison of FFT magnitude between PV panels can detect the arc fault condition.

C. Discuss About Arc Fault Location

The differential type voltage sensing method has simple arc fault detection algorithm using the voltage relationship of (8) and (9). This algorithm can detect the arc fault condition between

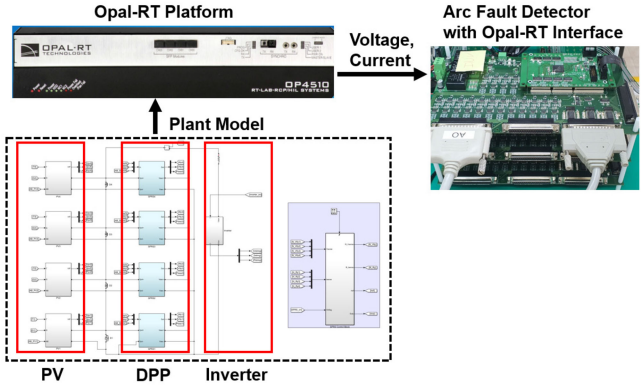

Fig. 8. Designed CHIL configuration.

TABLE I
DESIGN SPECIFICATION OF CHIL SYSTEM

parameters	values
number of PV panels	4
PV voltage range	27 V at MPPT 32 V at open
DPP converter	Bidirectional flyback converter
maximum power rating	1.29 kW

PV panels and between PV array and inverter. However, it cannot specify the exact location where the arc fault occurs. The common ground type sensing method is more complex than the differential type sensing method. When the arc fault occurs between PV arrays and an inverter, the voltage magnitude comparison using (8) and (9) can detect the arc fault condition. When arc fault occurs between PV panels, the frequency analysis using (16) and (17) can detect the arc fault condition. This algorithm can specify the exact location where arc fault occurs.

III. EXPERIMENTAL VERIFICATION

The voltage relationship according to the voltage sensing method and DPP operation are verified with the Control-HIL test-bed. Fig. 8 shows the configuration of Control-HIL, which can simulate a large number of PV panels and DPP operation. The real-time simulator (OP4510, Opal-RT) implements the plant model, which has four PV panels and DPP units, inverter, and arc fault model [7], [32], [34]. Table I shows the designed specification of CHIL system derived in (5).

Fig. 9(a) shows the Control-HIL experimental results for the differential type sensing. In the no arc fault condition, the total PV and dc-link voltages have same magnitude as derived in (5). In the arc fault condition, the total PV voltage is higher than the dc-link voltage of inverter according to the voltage drop caused by the arc fault as derived in (6). Fig. 9(b) shows the Control-HIL experimental results for the common ground type sensing. The arc fault occurs between PV4 and PV3, which induces the voltage drop in V_{DPP4}. Therefore, total PV voltage and dc-link voltage have same magnitude at no arc fault and arc fault conditions between PV panels. The voltage drop of PV

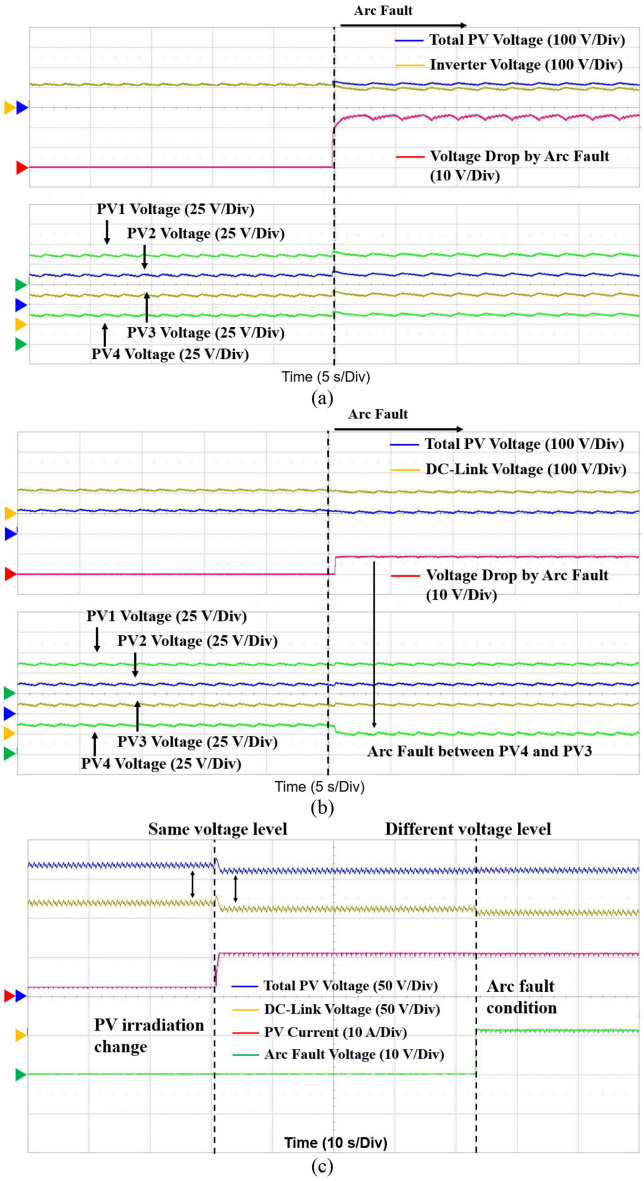

Fig. 9. Experimental results using CHIL. (a) Differential type sensing. (b) Common ground type sensing. (c) Power variation condition.

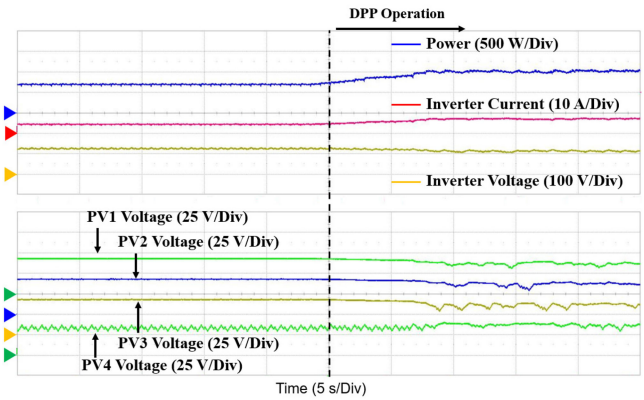

Fig. 10. Operational waveforms of DPP units.

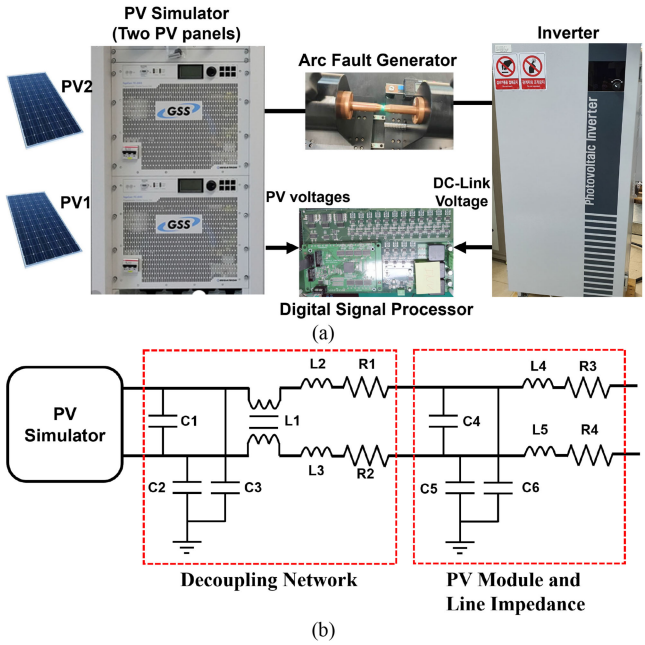

Fig. 11. Prototype test setup. (a) Configuration of arc fault test setup. (b) Equivalent circuit of PV module impedance.

contains the frequency response of arc fault condition, which is described in Fig. 5 using the experimental results. However, the control-HIL cannot show the frequency response of arc fault condition, because the limited time-step of simulation (10 μs).

Fig. 9(c) shows the voltage relationship comparison between power variation and arc fault condition using the differential type sensing method. The irradiation change of PV panel makes the power variation, which induces same voltage magnitude change of $V_{PV,tot}$ and V_{Link}. However, the arc fault condition induces a voltage difference between the total PV and dc-link voltages. Fig. 10 shows the operational waveform of DPP units, which implements the local MPPT for each PV panel [35]. The designed structure can obtain the arc fault detection and power generation improvement, which can improve the efficiency and safety of PV systems.

Fig. 11(a) shows the prototype testbed with PV simulators, arc fault generator, and an inverter, which can verify the arc fault detection performance. The arc fault generator is designed with the UL 1699B standard, which locates between PV arrays and between PV panel and inverter. Two PV simulators (TC.GSS.32.600.4WR.S, Regatron) are series connected to operate as two PV panels. The impedance network of Fig. 11(b) can simulate the real PV module using the PV simulator, which is designed with the UL1699B standard. The controller (TMS320F28277S, TI) receives the information of PV and inverter voltages for the arc fault detection. Table II shows the design specification of prototype PV systems.

Fig. 12(a) and (b) presents the arc fault condition and its detection according to the fault locations based on the differential type voltage sensing method. It verifies that the arc fault condition induces the voltage drop in the dc-link voltage of

TABLE II
DESIGN SPECIFICATION OF PROTOTYPE SYSTEM

Conditions	Parameter	Values
Number of PV panels		2
Case 1	PV voltage range	375 V at MPPT 426 V at open
	Maximum power rating	3.3 kW
	Arc gap	0.8 mm
	Arc generation speed	2.5 mm/sec
Case 2	PV voltage range	300 V at MPPT 376 V at open
	Maximum power rating	2.4 kW
	Arc gap	1.1 mm
	Arc generation speed	5 mm/sec
Case 3	PV voltage range	270 V at MPPT 335 V at open
	Maximum power rating	4 kW
	Arc gap	2.5 mm
	Arc generation speed	5 mm/sec

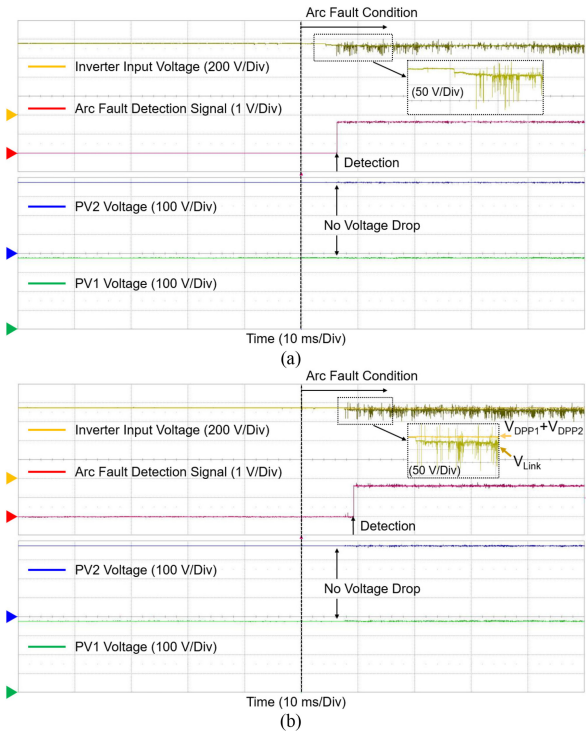

Fig. 12. Arc fault detection of differential type voltage sensing. (a) Arc fault between PV and inverter. (b) Arc fault between PV panels.

inverter compared to the total PV voltages measured by DPP units, as derived in (6). Based on (8) and (9), the algorithm of Fig. 4 can detect the arc fault condition according to the arc fault location.

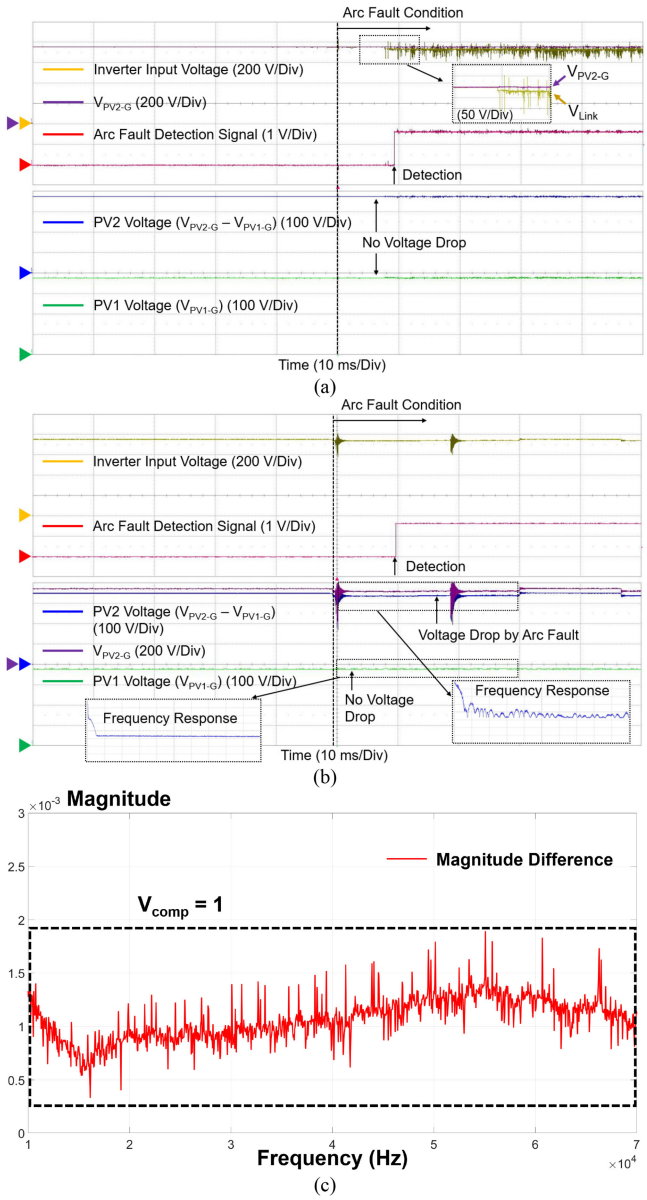

Fig. 13. Arc fault detection of differential type voltage sensing. (a) Arc fault between the PV and inverter. (b) Arc fault between PV panels. (c) FFT results under power variation.

Fig. 13(a) and (b) presents the arc fault detection according to the arc fault locations using the common ground type sensing method. Fig. 13(a) shows the arc fault condition between PV arrays and an inverter, which induces the voltage drop in the dc-link voltage of inverter compared to the total PV voltage. In this case, the voltage relationship using (8) and (9) can be used for arc fault detection. Fig. 13(b) shows the arc fault condition between PV panels, which has no voltage difference between total PV and dc-link voltages by the arc fault. This condition shows the arc fault between PV2 and PV1 panels, which results in the voltage drop caused by arc fault on V_{DPP2}. It verifies the relationship of (16) and (17). Fig. 5 shows the relative comparison of FFT magnitude between PV panels. The frequency domain analysis can detect the arc fault condition using the detection algorithm

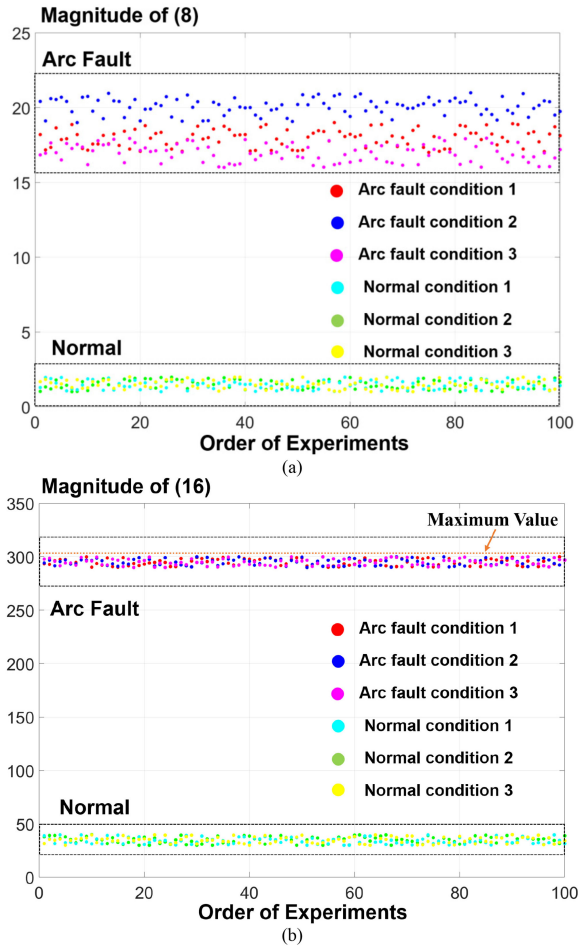

Fig. 14. Repetitive test results for proposed detection algorithm. (a) Performance of differential type voltage sensing. (b) Performance of common ground type voltage sensing.

of Fig. 7. Fig. 13(c) shows the frequency response of arc fault condition under the power variation condition in the case of the common ground type sensing method. The relative comparison of the FFT magnitudes of (14) and (15) helps in detecting the arc fault condition with a varying power.

The proposed arc fault detection algorithm has a fast detection speed less of than 100 ms, which satisfies the UL 1699B standard (2.5 s). In addition, the repetitive experiments can validate the sensitivity and safety of the proposed arc fault detection algorithm as follows [28]:

$$\text{Sensitivity} = \frac{TP}{TP + FN} \times 100\% \tag{21}$$

$$\text{Safety} = \frac{TN}{TN + FP} \times 100\% \tag{22}$$

where *TP* is the number of right arc fault detection, *TN* is the number of right normal condition detection, *FP* is the number of false detection of arc fault condition, and *FN* is the number of false normal condition detection. The sensitivity is the detection precision between the arc fault and normal condition. The safety is the fail-rate of arc fault detection. Fig. 14 shows the performance of voltage relationship of (8) and frequency domain analysis of (16). The arc fault detection algorithm can distinguish between a normal and arc fault conditions under the designed test condition. The proper threshold value selection can achieve 100 percent sensitivity and safety using (21) and (22).

IV. Conclusion

This article proposes the series dc arc fault detection algorithm employing the DPP structure, which can detect the arc fault condition between PV panels and between PV arrays and an inverter. The proposed algorithm uses the time domain and frequency domain analysis according to the voltage sensing structure of DPP units. It can improve the functionality of DPP units with integration of MPPT for each PV panel and arc fault detection. In addition, this method does not require the additional sensors for the arc fault detection, which can improve the cost-effectiveness of PV systems. The voltage relationship according to the arc fault condition and DPP operation is verified with the control-HIL test-bed. In addition, the proposed detection algorithm is verified with the prototype test-bed system. The arc fault is detected less than 100 ms, which can satisfy the UL 1699B standard.

References

[1] K. Jia, Z. Yang, Y. Fang, T. Bi, and M. Sumner, "Influence of inverter-interfaced renewable energy generators on directional relay and an improved scheme," *IEEE Trans. Power Electron.*, vol. 34, no. 12, pp. 11843–11855, Dec. 2019.

[2] Y. Wang, X. Lin, and M. Pedram, "A near-optimal model-based control algorithm for households equipped with residential photovoltaic power generation and energy storage systems," *IEEE Trans. Sustain. Energy*, vol. 7, no. 1, pp. 77–86, Jan. 2016.

[3] Y. Lu, K. Sun, H. Wu, X. Dong, and Y. Xing, "A three-port converter based distributed DC grid connected PV system with autonomous output voltage sharing control," *IEEE Trans. Power Electron.*, vol. 34, no. 1, pp. 325–339, Jan. 2019.

[4] L. B. G. Campanhol, S. A. O. da Silva, A. A. de Oliveira, and V. D. Bacon, "Power flow and stability analyses of a multifunctional distributed generation system integrating a photovoltaic system with unified power quality conditioner," *IEEE Trans. Power Electron.*, vol. 34, no. 7, pp. 6241–6256, Jul. 2019.

[5] Underwriters Laboratories (UL) 1699B, "Outline of investigation for 405 photovoltaic (PV) DC arc-fault circuit protection," no. 2, pp. 1–42, Jan. 2013.

[6] National Electrical Code (NEC), 2011 Edition, NFPA70, National Fire Protection Association, Quincy, MA, USA.

[7] M. Weerasekara, M. Vilathgamuwa, and Y. Mishra, "Modelling of DC arcs for photovoltaic system faults," in *Proc. IEEE 2nd Annu. Southern Power Electron. Conf.*, 2016, pp. 1–4.

[8] G. Parise, L. Martirano, and M. Laurini, "Simplified arc-fault model: The reduction factor of the arc current," in *Proc. IEEE Ind. Appl. Soc. Annu. Meeting*, 2012, pp. 1–6.

[9] M. Naidu, T. J. Schoepf, and S. Gopalakrishnan, "Arc fault detection scheme for 42-V automotive DC networks using current shunt," *IEEE Trans. Power Electron.*, vol. 21, no. 3, pp. 633–639, May 2006.

[10] C. He, L. Mu, and Y. Wang, "The detection of parallel arc fault in photovoltaic systems based on a mixed criterion," *IEEE J. Photovolt.*, vol. 7, no. 6, pp. 1717–1724, Nov. 2017.

[11] A. Shekhar, L. Ramírez-Elizondo, S. Bandyopadhyay, L. Mackay, and P. Bauera, "Detection of series arcs using load side voltage drop for protection of low voltage DC systems," *IEEE Trans. Smart Grid*, vol. 9, no. 6, pp. 6288–6297, Nov. 2018.

[12] Q. Lu, Z. Ye, M. Su, Y. Li, Y. Sun, and H. Huang, "A DC series arc fault detection method using line current and supply voltage," *IEEE Access*, vol. 8, pp. 10134–10146, 2020.

[13] E. Bauer, M. Troth, J. Wang, D. Schweickart, and D. Grosjean, "Optimal threshold selection and efficacy evaluation for a generic dc series arc detection algorithm," in *Proc. IEEE Nat. Aerosp. Electron. Conf.*, 2018, pp. 525–528.

[14] Y. Abdullah, B. Hu, Z. Wei, J. Wang, and A. Emrani, "Adaptive detection of DC arc faults based on hurst exponents and current envelope," in *Proc. IEEE Appl. Power Electron. Conf. Expo.*, 2018, pp. 3392–3397.

[15] J. Gu, D. Lai, J. Wang, J. Huang, and M. Yang, "Design of a DC series arc fault detector for photovoltaic system protection," *IEEE Trans. Ind. Appl.*, vol. 55, no. 3, pp. 2464–2471, May/Jun. 2019.

[16] Y. Zhang and L. Wang, "The research on characteristics of DC arc fault based on FRFT," in *Proc. 20th Eur. Conf. Power Electron. Appl.*, 2018, pp. 1–6.

[17] M. H. Riza Alvy Syafi'i, E. Prasetyono, M. K. Khafidli, D. O. Anggriawan, and A. Tjahjono, "Real time series DC arc fault detection based on fast fourier transform," in *Proc. Int. Electron. Symp. Eng. Technol. Appl.*, 2018, pp. 25–30.

[18] M. H. Riza Alvy Syafi'i, E. Prasetyono, M. K. Khafidli, D. O. Anggriawan, and A. Tjahjono, "Real time series DC arc fault detection based on fast fourier transform," in *Proc. Int. Electron. Symp. Eng. Technol. Appl.*, 2018, pp. 25–30.

[19] A. Maqsood, D. Oslebo, K. Corzine, L. Parsa, and Y. Ma, "STFT cluster analysis for DC pulsed load monitoring and fault detection on naval shipboard power systems," *IEEE Trans. Transp. Electrific.*, vol. 6, no. 2, pp. 821–831, Jun. 2020.

[20] X. Yao, L. Herrera, S. Ji, K. Zou, and J. Wang, "Characteristic study and time-domain discrete-wavelet-transform based hybrid detection of series DC arc faults," *IEEE Trans. Power Electron.*, vol. 29, no. 6, pp. 3103–3115, Jun. 2014.

[21] Z. Wang and R. S. Balog, "Arc fault and flash signal analysis in DC distribution systems using wavelet transformation," *IEEE Trans. Smart Grid*, vol. 6, no. 4, pp. 1955–1963, Jul. 2015.

[22] C.-H. Kim, H. Kim, Y.-H. Ko, S.-H. Byun, R. K. Aggarwal, and A. T. Johns, "A novel fault-detection technique of high-impedance arcing faults in transmission lines using the wavelet transform," *IEEE Trans. Power Del.*, vol. 17, no. 4, pp. 921–929, Oct. 2002.

[23] S. Liu, L. Dong, X. Liao, X. Cao, X. Wang, and B. Wang, "Application of the variational mode decomposition-based time and time–frequency domain analysis on series DC arc fault detection of photovoltaic arrays," *IEEE Access*, vol. 7, pp. 126177–126190, 2019.

[24] M. Wei *et al.*, "High impedance arc fault detection based on the harmonic randomness and waveform distortion in the distribution system," *IEEE Trans. Power Del.*, vol. 35, no. 2, pp. 837–850, Apr. 2020.

[25] S. Chen and X. Li, "PV series arc fault recognition under different working conditions with joint detection method," in *Proc. IEEE 62nd Holm Conf. Elect. Contacts*, 2016, pp. 25–32.

[26] V. Le, X. Yao, C. Miller, and B. Tsao, "Series DC arc fault detection based on ensemble machine learning," *IEEE Trans. Power Electron.*, vol. 35, no. 8, pp. 7826–7839, Aug. 2020.

[27] N. Qu, J. Zuo, J. Chen, and Z. Li, "Series arc fault detection of indoor power distribution system based on LVQ-NN and PSO-SVM," *IEEE Access*, vol. 7, pp. 184020–184028, 2019.

[28] S. Lu, T. Sirojan, B. T. Phung, D. Zhang, and E. Ambikairajah, "DA-DCGAN: An effective methodology for DC series arc fault diagnosis in photovoltaic systems," *IEEE Access*, vol. 7, pp. 45831–45840, 2019.

[29] Y. Jeon and J. Park, "Unit-minimum least power point tracking for the optimization of photovoltaic differential power processing systems," *IEEE Trans. Power Electron.*, vol. 34, no. 1, pp. 311–324, Jan. 2019.

[30] Y. Jeon and J. Park, "Unit-minimum least power point tracking for the optimization of photovoltaic differential power processing systems," *IEEE Trans. Power Electron.*, vol. 34, no. 1, pp. 311–324, Jan. 2019.

[31] C. Olalla, C. Deline, D. Clement, Y. Levron, M. Rodriguez, and D. Maksimovic, "Performance of power-limited differential power processing architectures in mismatched PV systems," *IEEE Trans. Power Electron.*, vol. 30, no. 2, pp. 618–631, Feb. 2015.

[32] K. A. Kim, P. S. Shenoy, and P. T. Krein, "Converter rating analysis for photovoltaic differential power processing systems," *IEEE Trans. Power Electron.*, vol. 30, no. 4, pp. 1987–1997, Apr. 2015.

[33] Y. Jeon, H. Lee, K. A. Kim, and J. Park, "Least power point tracking method for photovoltaic differential power processing systems," *IEEE Trans. Power Electron.*, vol. 32, no. 3, pp. 1941–1951, Mar. 2017.

[34] M. Kim, S. Kwak, K. A. Kim, and J. Jung, "Enhanced computation performance of photovoltaic models for power Hardware-in-the-loop simulation," *IEEE Trans. Ind. Electron.,* early access.

[35] S. Park *et al.*, "Design methodology of bidirectional flyback converter for differential power processing modules in PV applications," in *Proc. 10th Int. Conf. Power Electron. ECCE Asia*, 2019, pp. 1759–1764.

Hwa-Pyeong Park (Member, IEEE) was born in Gimcheon, South Korea, in 1991. He received the Ph.D. degree in electrical engineering from the Ulsan National Institute of Science and Technology, Ulsan, South Korea, in 2019.

He is currently working in Korea Institute of Energy Research (KIER), Energy Efficiency Division. His main research interests include high-power-density dc–dc converters, power control algorithm for power converters, and battery management systems.

Mina Kim (Student Member, IEEE) was born in Ulsan, South Korea, in 1992. She received the B.S. degree in electronic and electrical engineering in 2015 from the Ulsan National Institute of Science and Technology, Ulsan, South Korea, where she is currently working toward the Ph.D. degree in electrical and computer engineering.

Her main research interests include dc–dc resonant converters, wireless power transfer technology, and power hardware in-the-loop simulation.

Jee-Hoon Jung (Senior Member, IEEE) was born in Suwon, South Korea, in 1977. He received the B.S. degree in electrical engineering and the M.S. and Ph.D. degrees in electrical and computer engineering from the Department of Electronics and Electrical Engineering, Pohang University of Science and Technology, Pohang, South Korea, in 2000, 2002, and 2006, respectively.

From 2006 to 2009, he was a Senior Research Engineer with the Digital Printing Division, Samsung Electronics Company Ltd., Suwon. From 2009 to 2010, he was a Postdoctoral Research Associate with the Department of Electrical and Computer Engineering, Texas A&M University at Qatar, Doha, Qatar. From 2011 to 2012, he was a Senior Researcher in the Power Conversion and Control Research Center, HVDC Research Division, Korea Electrotechnology Research Institute, Changwon. Since 2013, he has been involved as a Faculty Member in Electrical Engineering, Ulsan National Institute of Science and Technology (UNIST), Ulsan, where he is presently working as an Associate Professor. His current research interests include dc/dc and ac/dc converters, switched-mode power supplies, digital control and signal processing algorithms, power conversion for renewable energy, and real-time and power hardware-in-the-loop (HIL) simulations of renewable energy and power grids. Recently, he has been researching high-frequency power converters using wide bandgap devices, bidirectional power converters for smart grids, power control algorithms, spread spectrum techniques, and power line communications for dc microgrids, induction heating techniques for home appliances and industrial applications, and artificial intelligence techniques applied to Power Electronics area.

Dr. Jung is a Senior Member of the IEEE Industrial Electronics Society, the IEEE Power Electronics Society, the IEEE Industry Applications Society (IAS), and the IEEE Power and Energy Society. He has served as an Asian Liason Officer for the Industrial Power Converter Committee in the IEEE IAS, a Member of the Editorial Committee of the Korea Institute of Power Electronics (KIPE), and an Associate Editor of the Journal of Power Electronics (JPE). He is currently serving as a Member of the Board of Directors of the KIPE and an Editorial Board Member for Energies in the Multidisciplinary Digital Publishing Institute (MDPI).

Suyong Chae (Member, IEEE) received the B.S. and M.S. degrees in electrical engineering from the Korea Advanced Institute of Science and Technology, Daejeon, South Korea, in 1998 and 2000, respectively, and the Ph.D. degree in electrical engineering from the Seoul National University, Seoul, South Korea, in 2009.

From 2000 to 2010, he was a Research Engineer with Samsung SDI. He has been a Principle Researcher with the Korea Institute of Energy Research, Daejeon, South Korea, since 2010. His current research interests include power electronics, modeling, and control of distributed power system.